Int. J. Electrochem. Sci., 15 **(2020)** 10104 – 10116, doi: 10.20964/2020.10.41

International Journal of ELECTROCHEMICAL SCIENCE
www.electrochemsci.org

Decreasing Weight Particle Swarm Optimization Combined with Unscented Particle Filter for the Non-Linear Model for Lithium Battery State of Charge Estimation

Lei Chen, Shunli Wang[*]*, Hong Jiang, Carlos Fernandez, Chunyun Zou*

School of Information Engineering, Southwest University of Science and Technology, Mianyang 621010
[*]E-mail: 497420789@qq.com

Received: 5 June 2020 / *Accepted:* 20 July 2020 / *Published:* 31 August 2020

Accurate estimation of State of Charge (SOC) of wireless sensor network nodes is of great significance for wireless sensor network layout. A combination strategy method based on unscented particle filter using weight particle swarm optimization (PSO-UPF) algorithm is proposed to improve estimation accuracy. The particle filter (PF) algorithm is usually used to deal with nonlinear problems, easily falling into particle degeneration and particle shortage. The unscented particle filter (UPF) algorithm can overcome the shortcomings by using the unscented Kalman filter (UKF) to generate the importance density function. Meanwhile, the particle swarm optimization (PSO) algorithm could improve the resampling process to solve particle shortage. Thus, the combination strategy improves the importance density function and the resampling method simultaneously. With the simulation comparison of PF, UPF and PSO-UPF algorithms, the results show that the proposed algorithm has higher estimation accuracy with the root mean square error less than 1%. Furthermore, the proposed algorithm could achieve good accuracy with few particles, which could save running time and improve the estimate efficiency.

Keywords: State of Charge; particle filter; unscented particle filter; linearly decreasing weight particle swarm optimization

1. INTRODUCTION

Wireless Sensor Network (WSN) is an advanced developing technology to monitor and record the physical or environmental conditions, such as temperature, wind, pollution levels, and so on [1]. The WSN is usually equipped with large number of nodes, which can communicate with each other using radio signals [2, 3]. The nodes are small size, low price, multi-function and eco-friendly which can meet the requirement of lithium battery [4]. WSN nodes can be placed randomly in every corner of monitoring area while the power supply and maintenance are significantly compromised by the harsh

environment [5]. It is important to monitor remaining energy in the battery and estimate battery life timely to reasonably plan the use of each node. To evaluate the performance of battery, it is highly desirable to estimate the real-time state of charge (SOC) of lithium battery [6, 7].

For the problem of nonlinear state estimation, the expression of posterior probability density can't be obtained directly, and only two kinds of approximate methods can be used [8-12]. Extended Kalman filter method is used to linearize the nonlinear model via Taylor equation calculation [13]. However, it probably results in Kalman filters divergence [14]. The other method is to approximate the posterior probability density distribution, i.e. UKF and PF [15-21]. For the UKF model, it can be used to deal with nonlinear transfer of mean and covariance to obtain high accuracy. PF approximates the posterior probability density distribution through the weight values of particles, and is suitable for nonlinear non-Gaussian model [22-25]. Nevertheless, it tends to eliminate particles with low weights due to particle depletion on basic of sequential importance sampling (SIS) algorithm. Until now scientists have made many efforts to solve the defects via modifying the importance density function and resampling process [26-29]. In Ref. [30-32], the UPF algorithm is proposed to overcome particle degeneration in a certain extent. However, the accuracy is significantly compromised by particle scarcity. Ahwiad group reported an enhanced mutation particle filtering (EMPF) to improve the performance of PF by generating mutated particles from prior particles to represent the high-likelihood area more sufficiently [33]. Genetic algorithm was introduced to increase the diversity of particles and improve smaller weight particles [34]. UPF is proposed on basic of linear optimization combination resampling (U-LOCR-PF) to solve coefficient of uncertain correlation step [35]. Then, Lin proposed PSOPF algorithm which combines particle swarm optimization (PSO) with PF algorithm to generate particles diversity [36]. However, it still exist some defects [37-42]. As mentioned above, new algorithms for accurate estimation of SOC are highly desired.

The main contribution of this study is to present a linear decreasing weight particle swarm optimization algorithm on basic of the PF and UKF algorithm. UKF is used to sample particles and generate the importance density function of PF, effectively alleviate particle degeneration. PSO is introduced to improve the resampling process of UPF, which can increase the diversity of particles, enhance the calculation efficiency, and remit particle shortage problem to a certain extent. Thus, the combination strategy improves the importance density function and the resampling method.

2. THEORY AND METHOD RESEARCH

2.1. Improved equivalent circuit model

Lithium battery equivalent modeling is the basis of SOC estimation, and the common equivalent circuit models include Rint model, RC model, Thevenin model and PNGV model. In this paper, the improved equivalent circuit model (IECM) is used as the equivalent circuit model of lithium battery to afford accurate estimation of SOC, which consists of ohmic internal resistance module, RC module and open circuit voltage module (shown in Fig. 1). The ohmic internal resistance is divided

into benchmark ohmic internal resistance and charge/discharge differential ohmic internal resistance to simulate the characteristic change of ohmic internal resistance of charging/discharging.

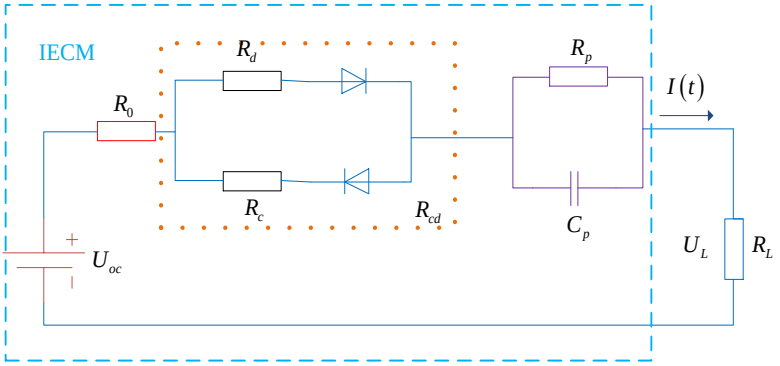

Figure 1. The improved equivalent circuit model

U_{oc} represents the open circuit voltage of the battery. R_0 represents the benchmark ohmic internal resistance. R_{cd} characterizes the internal resistances of R_c and R_d at the time of charge and discharge. R_p represents the polarization resistance and C_p represents the polarization capacitance. U_L is the closed-circuit voltage when the battery is connected to the external circuit. According to Kirchhoff's law, the voltage and current expressions of the circuit can be obtained as:

$$\begin{cases} U_L = U_{oc} - U_o - U_{cd} - U_p \\ I(t) = C_p \dfrac{dU_p}{dt} + \dfrac{U_p}{R_p} \end{cases} \quad \text{..... (1)}$$

Based on the definition of SOC, the equivalent circuit model is discretized. The operating current I is the input of the system, and the battery terminal voltage U_L is the observation state. In order to get closer to the real condition, the process noise and observation noise of the system are added, and the state space equation after discretization is obtained as follows:

$$\begin{cases} \begin{bmatrix} SOC_{k+1} \\ U_{p,k+1} \end{bmatrix} = \begin{bmatrix} 1 & 0 \\ 0 & e^{-\frac{\Delta t}{\tau}} \end{bmatrix} \begin{bmatrix} SOC_k \\ U_{p,k} \end{bmatrix} + \begin{bmatrix} -\dfrac{\eta \Delta t}{Q} \\ R_p\left(1 - e^{-\frac{\Delta t}{\tau}}\right) \end{bmatrix} I_k + \omega_k \\ U_{L,k} = U_{OC(SOC_k)} - [0 \quad 1][SOC_k \quad U_{p,k}]^T - R_0 I_k - R_{cd} I_k + v_k \end{cases} \quad \text{..... (2)}$$

The parameters [R_0, R_d, R_c, R_p, C_p] need to be identified by the hybrid pulse power characterization (HPPC). The off-line parameter identification of the battery model is carried out in this paper.

2.1. Particle filter

Particle filtering algorithm is an approximate numerical solution method on basic of Bayesian estimation and Monte Carlo method. A series of sampling points (like ‘particles’) are used to represent

the state distribution, calculate discrete probability density functions, and replace the average of particles integral over continuous space in order to minimize square error. In practice for PF algorithm, the SIS method is introduced to obtain an approximate posterior probability density function. When PF is applied to SOC estimation of lithium battery, the state equation and observation equation are listed as below:

$$\begin{cases} SOC_{k+1} = f(SOC_k) + \omega_k \\ U_{L,k} = h(SOC_k) + \upsilon_k \end{cases} \quad \text{..... (3)}$$

SOC_{k+1} and SOC_k represent the SOC value at current and previous time respectively, and the battery terminal voltage U_L is the observation state. To understand the work mechanism of PF filter, the flow chart is shown in Fig. 2.

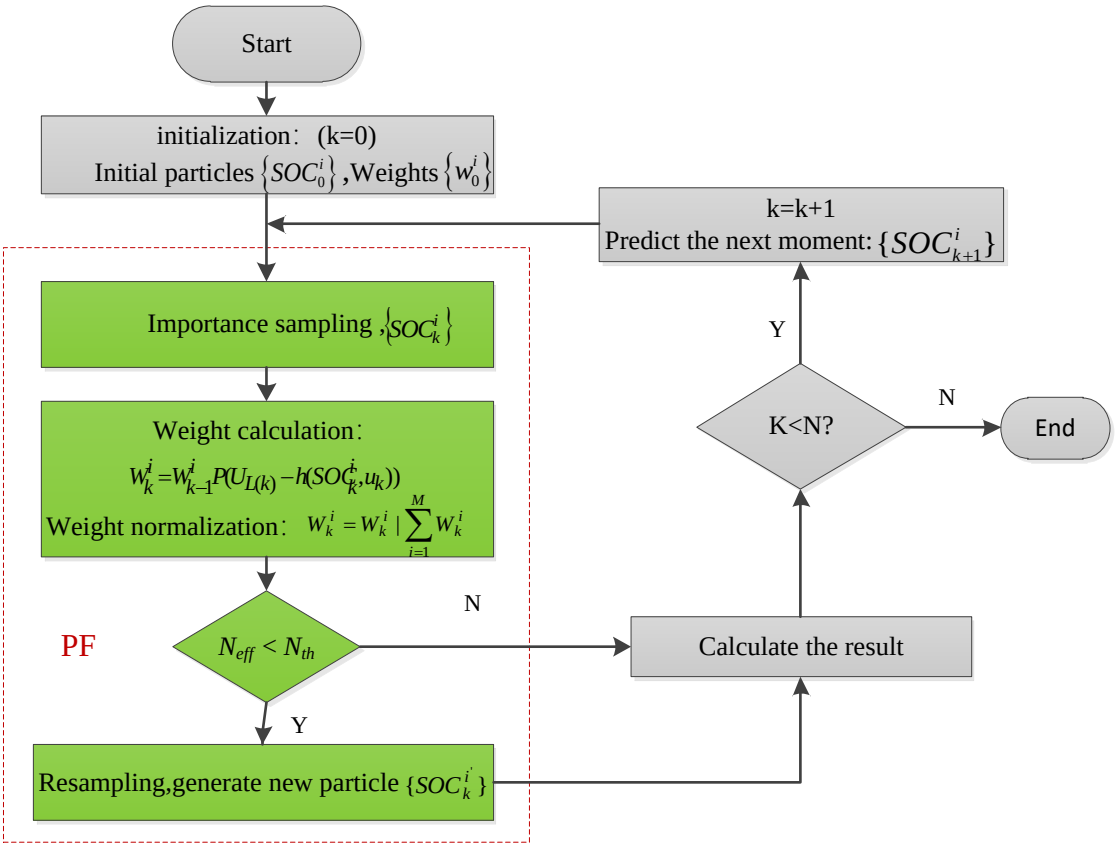

Figure 2. Flow diagram of the PF

The main implementation steps are shown as below:

Step1. Initialization:

$P(x_0)$ is the prior probability distribution, and SOC initial particles are randomly generated.

Step2. Importance sampling: Collecting sample set from the importance density function:

$SOC_k^i \sim q(x_k^{(i)} \mid x_{k-1}^{(i)}, y_{1:k}) : p\left(x_k^{(i)} \mid x_{k-1}^{(i)}\right)$

Step3. Weight calculation and normalization:

$$w_k^i = w_{k-1}^i p(y_k \mid SOC_k^i) \quad \text{..... (4)}$$

$$w_k^i = w_k^i / \sum_{i=1}^{M} w_k^i \quad \text{..... (5)}$$

Step4. Selection stage (resampling): Calculating effective particle numbers:

$$N_{eff} = 1 \Big/ \sum_{i=1}^{M} (w_k^i)^2 \quad \text{..... (6)}$$

If $N_{eff} < N_{th}$ (N_{th} is the threshold of particle number), resampling is conducted to generate a new sample set, otherwise, turn to step5.

Step5. Outputting the estimation:

$$SOC_k = \sum_{i=1}^{M} w_k^i SOC_k^i \quad \text{..... (7)}$$

2.3. Unscented particle filter using linearly decreasing weight particle swarm optimization

2.3.1. Unscented particle filter

In PF algorithm, the particle degeneration is observed when the likelihood function is in a narrow state, or the observation probability is located at the tail of the prior distribution. To solve the drawbacks, it is significant to find an optimal importance density function to transfer sample points in prior distribution area to the maximum likelihood area, so as to improve effective particles and approximate to the posterior probability density function. As shown in Fig. 3, UPF method is introduced to solve the defects of PF. UKF algorithm is used to select importance density function on basic of the UT transformation. It is used to calculate the mean value and variance of the particle set , and further to sample and update the particles, increase the overlap between the number of particles and the likelihood distribution during sampling. Finally, it makes the selection of particles closer to the observation value interval, and improves the filtering accuracy.

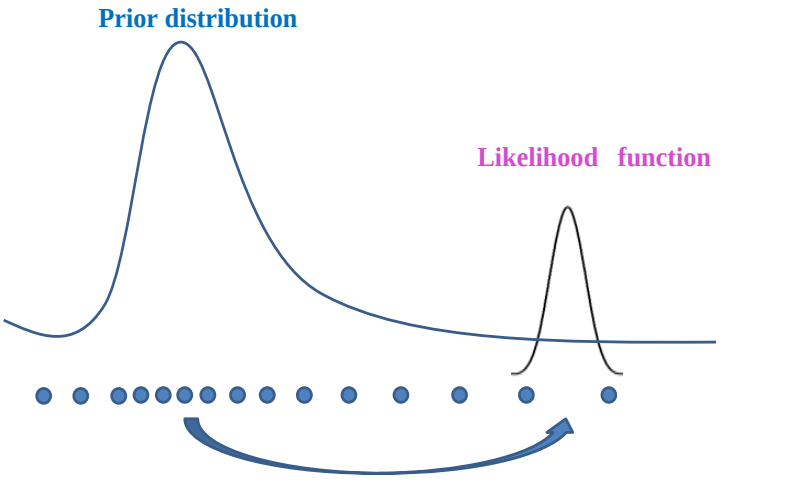

Figure 3. Mechanism of UPF algorithm

2.3.2. Weight particle swarm optimization

To overcome the lackage of particles in the resampling process, PSO is introduced into UPF through moving the particles globally during iteration process to search for and update the optimal particle position in the importance density function. So each particle could continuously move to the optimal position and approximate to the real value of the system, which solves the particle shortage phenomenon. The inertia weight coefficient ω is one of the important parameters that affect the performance of the PSO algorithm. The larger ω will increase the global search capability of the PSO, and the smaller one will increase the local search capability of the PSO. In this paper, linear decreasing weight is selected to update the inertial weight coefficient to balance the global and local search capabilities of particle swarm optimization. The main process of PSO-UPF is shown in Fig. 4:

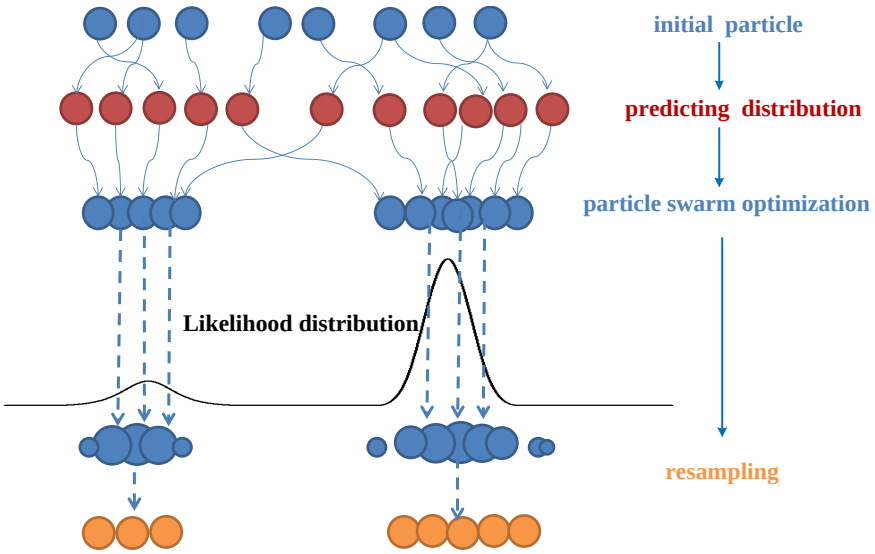

Figure 4. Mechanism of PSO algorithm

On the basis of lithium battery SOC estimation using PF, PSO-UPF algorithm is introduced to improve both the importance density function and the resampling process. The structure diagram of PSO-UPF algorithm is obtained in Fig. 5.

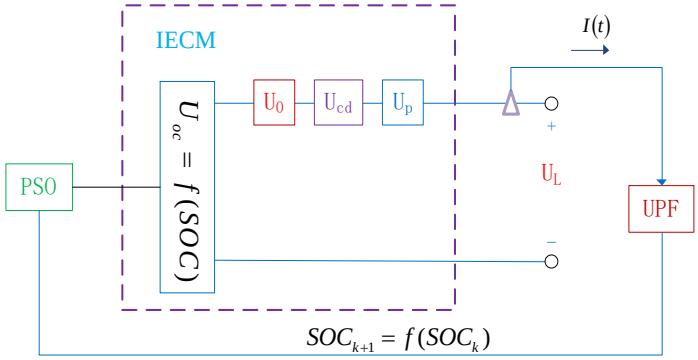

Figure 5. The structure of the UPF and PSO joint algorithm

The basic idea of the algorithm is: firstly, a group of SOC initial particles are generated according to the prior probability of the system state variable. Then UPF algorithm is taken to generate a new importance density function, and the output of UPF algorithm is taken as the input of PSO algorithm. The optimal estimation value is obtained to approach the current real SOC value through modification the original experience of conditional distribution. The optimal PSO-UPF algorithm is designed on the basic of following idea as shown in Fig. 6.

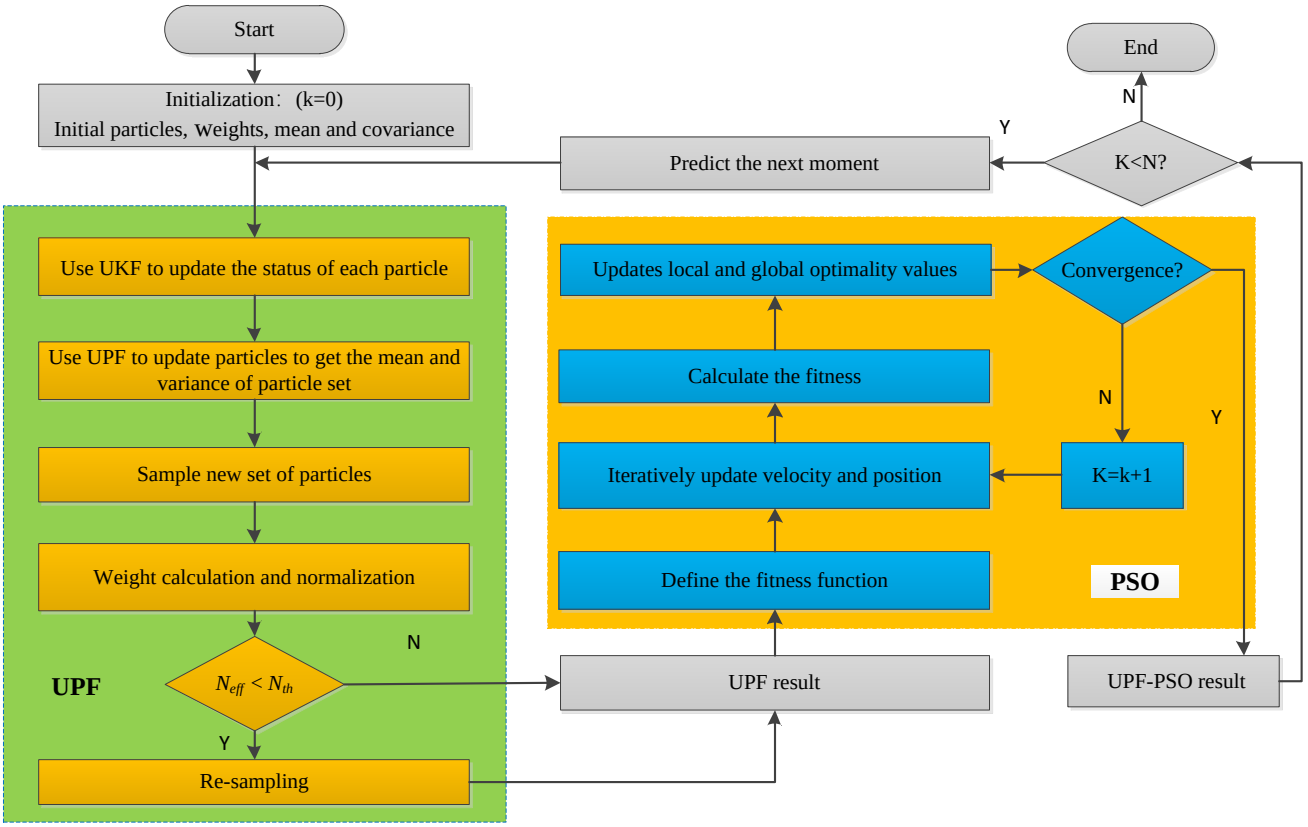

Figure 6. Flow diagram of the PSO-UPF

The main implementation steps are shown as below:

Step1. Initialization:

$p(x_0)$ is the prior probability distribution, and SOC initial particles are randomly generated. Particle weight is 1/M, and the initial mean value and covariance of the particle set is produced.

Step2. Importance sampling:

(1) UKF algorithm is used to update the sample set;

(2) Calculating the mean value and variance of the particle set obtained by UPF algorithm;

(3) Sample new set of particles from the importance density function:

$$SOC_k^i \sim q(x_k^{(i)} \mid x_{k-1}^{(i)}, y_{1:k}) : N(\overline{SOC_k^i}, \overline{P_k^i})$$

Step3. Weight calculation and normalization:

$$w_k^i = w_{k-1}^i p(y_k \mid \overline{SOC_k^i}) \quad \text{..... (8)}$$

$$w_k^i = w_k^i / \sum_{i=1}^{M} w_k^i \quad \text{..... (9)}$$

Step4. Selection stage (resampling): Calculating effective particle numbers:

$$N_{eff} = 1 \Big/ \sum_{i=1}^{M} (w_k^i)^2 \quad \text{..... (10)}$$

If $N_{eff} < N_{th}$ (N_{th} is the threshold of particle number), resampling is conducted to generate a new particle set, otherwise, turn to step 6.

Step5. Particle swarm optimization:

(1) Define the fitness function:

$$fitness = \exp[-\frac{1}{2R}(\mathrm{U}_{L,k} - h(\overline{SOC_k^i}, u_k)^2] \quad \text{..... (10)}$$

The value of the fitness function is essentially the weight of the particles to calculate the fitness. Then, it will choose the optimal values of the particle to update the position.

(2) Take the sample set generated by UPF as the initial position of PSO.

(3) Formula (12) is used to update the speed and position of each particle iteratively and calculate the fitness value of each particle. According to the fitness value, the local and global optimal values of the particle are updated to make the particle get closer to the real value.

$$\begin{cases} v_{k-1}^i = \omega * v_{k-1}^i + c_1 \mid randn \mid (p_{pbest} - x_{k-1}^i) + c_2 \mid randn \mid (p_{gbest} - x_{k-1}^i) \\ x_k^i = \mathrm{x}_{k-1}^i + \upsilon_{k-1}^i \end{cases} \quad \text{..... (12)}$$

ω is the inertia weight coefficient, c_1, c_2 is the learning factor, P_{pbest} is the local optimal value, P_{gbest} is the global optimal value.

(4) When the maximum number of iterations is reached, the search is stopped.

Step6. Outputting the estimation:

$$SOC_k = \sum_{i=1}^{M} w_k^i SOC_k^i \quad \text{..... (13)}$$

3. EXPERIMENTAL ANALYSIS

3.1. Parameter identification results

The parameters to be identified in this model include [R_0, R_d, R_c, R_p, C_p]. HPPC is used in this experiment. In order to explain the mechanism of HPPC experiment, a single HPPC pulse experiment is taken for analysis.

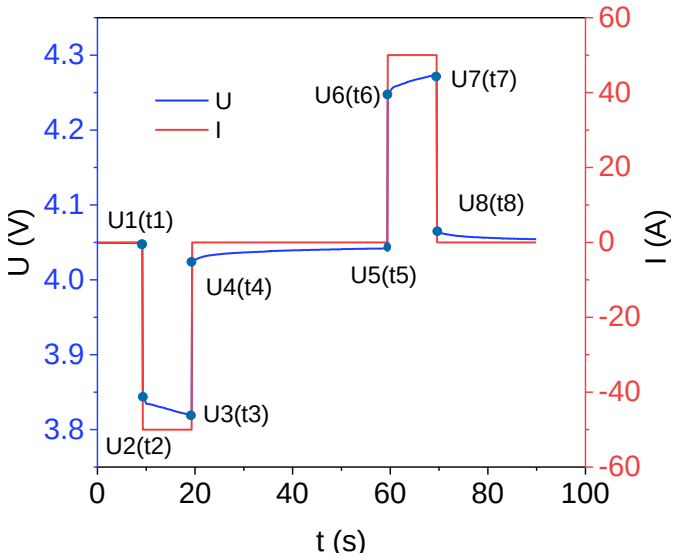

Figure 7. HPPC experimental voltage

As shown in Fig. 7, the voltage transient decreased which is caused by R_0 from *U1* to *U2*. Then the polarization capacitor C_p in the resistance-capacitance network is charged, showing that the voltage decreased slowly output a zero-input response from *U2* to *U3*. The terminal voltage enhancement and decrease is attributed to ohmic internal resistance of lithium-ion batteries during pulse charging and discharging. R_d and R_c are used to represent the differences. The calculation formula of ohm internal resistance can be calculated by formula 14;

$$\begin{cases} R_o = \dfrac{U_1 - U_2}{I} \\ R_d = \dfrac{U_3 - U_4}{I} - R_0 \\ R_c = \dfrac{U_7 - U_8}{I} - R_0 \end{cases} \quad \text{..... (14)}$$

U_1, U_2, U_3, U_4, U_7 and U_8 are shown in Fig. 7. R_0 represents the benchmark ohmic internal resistance, R_d is the discharge resistance, R_c is the charging resistance. The KVL circuit expression can be obtained by IECM. The parameters of each SOC point are identified by curve fitting to give the values of [R_0, R_d, R_c, R_p, C_p]. Finally, the relationship between the identification parameters and SOC is measured by means of polynomial fitting (formula 15):

$$U_L = U_{OC} - IR_0 - IR_{cd} - IR_p(1 - e^{-\frac{t}{\tau}}) \qquad (15)$$

3.2. Simulation analysis

To verify the feasibility of proposed PSO-PF algorithm for SOC estimation, the parameter function is identified to simulate the current change in the actual discharge process using Matlab

algorithm. The three algorithms of PF, UPF and PSO-UPF are measured to simulate from the three aspects of estimation accuracy, stability and running time for filter estimates in case of M = 20 and M = 100, respectively.

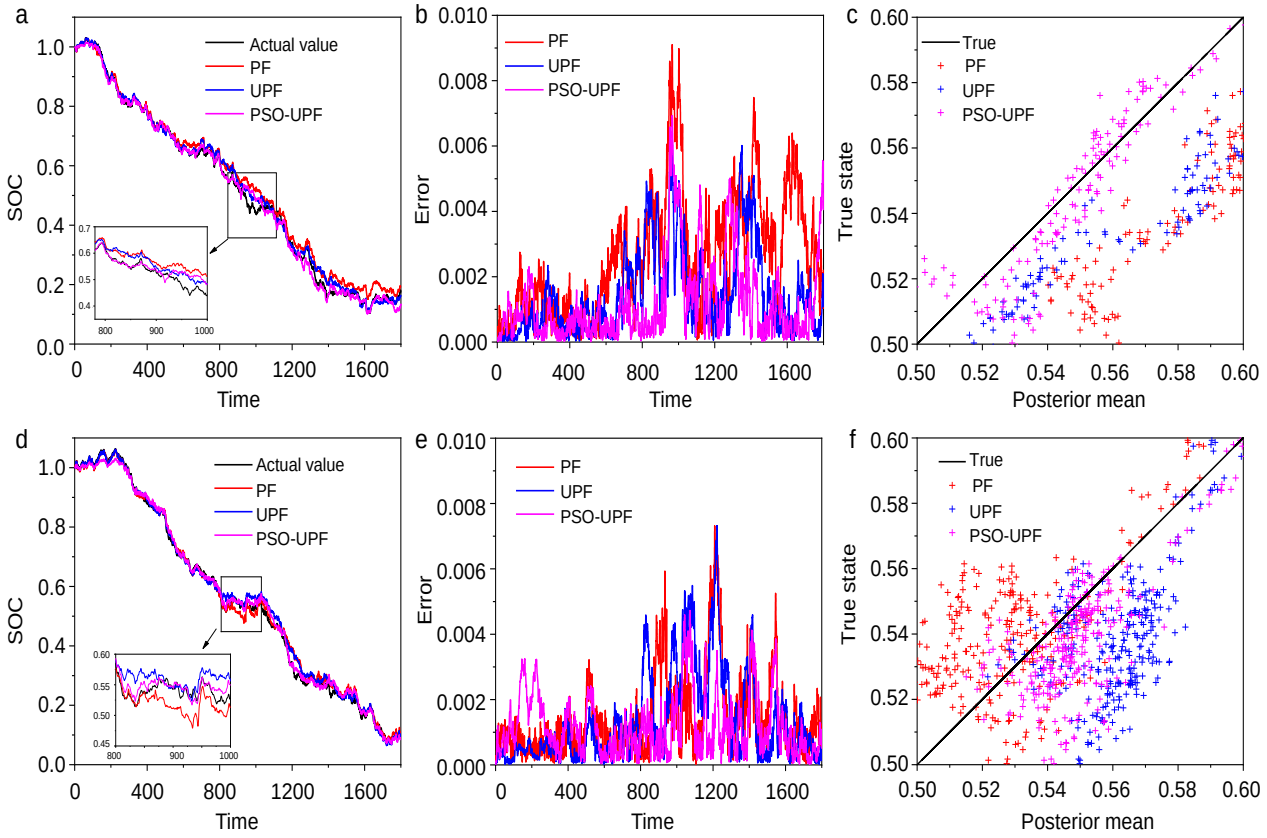

Figure 8. The three algorithms of PF, UPF and PSO-UPF for filter estimates in case of M = 20 (a) and 100 (d) of particles. The state deviation of three algorithms in case of M = 20 (b) and 100 (e) of particles. Posterior mean and real value analysis of PF, UPF and PSO-UPF under different M = 20 (c) and 100 (f) of particles

As shown in (Figs. 8a and 8d), it implied that all three algorithms provided the good filtering effect for SOC estimation. Moreover, it can be seen from the local amplification at time interval [800 1000] that each estimation method can well follow the change of the real value, and estimation accuracy is better in presence of more numbers of particles.

As shown in (Figs. 8b and 8e), the SOC estimation method based on PSO-UPF showed a significant improvement in estimation error compared with the other methods, and the estimation effect is more stable.

As shown in (Figs.8c and 8f), the PSO-UPF algorithm showed the best performance of posterior mean, which showed that accurate simulation did not rely on particle number. However, both the UPF and PF showed scattered distribution of particle and large error in case of few particles. With the increase of particle number, they got closer to the real value.

In order to evaluate the performance of the algorithm, the root mean square error (RMSE) and mean absolute error (MAE) of SOC estimation is defined though following formula:

$$\begin{cases} RMSE = \sqrt{\dfrac{\sum_{k=1}^{N}(SOC_k - SOC_{real,k})^2}{N}} \\ MAE = \dfrac{1}{N}\sum_{k=1}^{N}\left|(SOC_k - SOC_{real,k})\right| \end{cases} \quad \text{..... (16)}$$

N represents the running time of an experiment, SOC_k represents the estimated value of SOC in step k, and $SOC_{real,k}$ represents the real value size of SOC in step k.

Table 1 and table 2 compared the performance and running time of the three algorithms under different particle numbers, respectively.

Table 1. Performance comparison of three algorithms under different sample particle numbers

Three kinds of algorithms	Performance comparison of different sample particle Numbers			
	Number of particles M=20		Number of particles M=100	
	RMSE (%)	MAE （%）	RMSE (%)	MAE （%）
PF	1.87%	2.59%	1.27%	1.41%
UPF	1.43%	1.46%	1.40%	1.35%
PSO-UPF	1.27%	1.20%	0.94%	1.17%

Table 2. Running time comparison of three algorithms under different sampling particle numbers

Three kinds of algorithms	Running time /s comparison of different sample particle Numbers	
	Number of particles M=20	Number of particles M=100
PF	0.001045	0.003003
UPF	0.002821	0.009656
PSO-UPF	0.007445	0.096748

As shown in table 1, the RMSE and MAE of all the three algorithms decrease with the increase of the number of particles. The RMSE of PF and UPF algorithms indicated the accuracy is significantly improved depending on the number of particles. In the case of the same number of particles, PSO-UPF showed the highest accuracy and the best stability. The results confirmed that the selection of the particle number directly affected the accuracy of the filter.

The RMSE of PSO-UPF algorithm is less than 1%. Compared with the PF algorithm [14], where the MAE and RMSE of SOC estimation are 2.3% and 3.1% respectively, which showed the lower accuracy. The literature [20]estimated the SOC of EKF, EPF, CPF and UPF algorithms, and concluded that the UPF algorithm has the highest accuracy under noisy environment, with the MAE of 0.9%, but the accuracy of RMSE is not mentioned. There are a lot of improved algorithms around UPF. The paper[31] proposed GA-UPF algorithm, where the MAE is about 2%, and RMSE is about 0.9%.

This paper is based on PSO-UPF algorithm, where the MAE is 1.17%, and RMSE is 0.94%, which verified the feasibility of the algorithm.

In the case of few particles, the difference between PF algorithm and real value is large. The estimation accuracy of the PSO-UPF algorithm is higher than the other methods and very close to the real state as the PSO-UPF algorithm could effectively improve particle behavior and optimize particle position when the number of particles was limited. The enhanced effect of each sampled particle can be well distributed around the true value. The PSO-UPF algorithm does not require a large particle number to achieve good accuracy, which can save the running time and improve the efficiency of the algorithm.

4. CONCLUSIONS

In conclusion, we designed the IECM method using PSO-UPF algorithms to evaluate estimation of SOC of lithium batteries. By virtue of PSO-UPF algorithms, the importance density function of PF is generated by UKF to optimize the position and weight of particles and increase the number of sampling particles during resampling process. Compared with the PF, PSO-UPF allowed UPF and PSO to remit problem of particle degeneration and particle scarcity. The HPPC is used to identify the parameters and obtain the relationship between the model parameters and the SOC of lithium batteries. In comparison to the performance of three algorithms, PSO-UPF algorithm revealed the highest estimation accuracy in case of few/large number of particles and best robustness in practice application.

References

1. S. P. Maruthi, T. Panigrahi and R. P. K. Jagannath, *Expert Syst. Appl.*, 144 (2020).
2. C. Zygowski and A. Jaekel, *Ad Hoc Networks*, 96 (2020).
3. S. Narayanaswamy, S. Schlueter, S. Steinhorst, M. Lukasiewycz, S. Chakraborty and H. E. Hoster, *ACM Trans. Des. Autom. Electron. Syst.*, 21 (2016) 1.
4. K. Vijayalakshmi and P. Anandan, *Cluster Comput*, 22 (2019) 12275.
5. R. Senthilkumar and G. M. Tamilselvan, *J.Circuit Syst Comp*, 28 (2019).
6. T. Kalogiannis, M. S. Hosen, M. A. Sokkeh, S. Goutam, J. Jaguemont, L. Jin, G. Qiao, M. Berecibar and J. Van Mierlo, *Energies*, 12 (2019).
7. M. S. H. Lipu, M. A. Hannan, A. Hussain and M. H. M. Saad, *J. Renewable Sustainable Energy*, 9 (2017).
8. J. Sun, Q. Ma, R. Liu, T. Wang and C. Tang, *Int. J. Energy Res.*, 43 (2019) 7672.
9. T. Sun, B. Xia, Y. Liu, Y. Lai, W. Zheng, H. Wang, W. Wang and M. Wang, *Energies*, 12 (2019).
10. Y. Tian, D. Li, J. Tian and B. Xia, *Electrochim. Acta*, 225 (2017) 225.
11. Z. Xi, M. Dahmardeh, B. Xia, Y. Fu and C. Mi, *IEEE Trans. Veh. Technol.*, 68 (2019) 8613.
12. B. Xia, R. Huang, Z. Lao, R. Zhang, Y. Lai, W. Zheng, H. Wang, W. Wang and M. Wang, *Energies*, 11 (2018).
13. B. Duan, Q. Zhang, F. Geng and C. Zhang, *Int. J. Energy Res.*, 44 (2020) 1724.
14. B. Xia, S. Guo, W. Wang, Y. Lai, H. Wang, M. Wang and W. Zheng, *Energies*, 11 (2018).
15. B. Li, K. Peng and G. Li, *J. Renewable Sustainable Energy*, 10 (2018).

16. G. Li, K. Peng and B. Li, *J. Power Electron.*, 18 (2018) 129.
17. L. Li, A. A. F. Saldivar, Y. Bai and Y. Li, *Energies*, 12 (2019) 2784.
18. Y. Ma, Y. Chen, X. Zhou and H. Chen, *IEEE Trans. Control Syst. Technol.*, 27 (2019) 1788.
19. B. Peng, F. Zhang, J. Liang, L. Ding and Q. Wu, *Int. J. Electr. Power Energy Syst.*, 113 (2019) 251.
20. B. Xia, Z. Sun, R. Zhang, D. Cui, Z. Lao, W. Wang, W. Sun, Y. Lai and M. Wang, *Energies*, 10 (2017) 1149.
21. G. Xie, X. Peng, X. Li, X. Hei and S. Hu, *Can. J. Chem. Eng.*, (2019).
22. W. Qin, H. Lv, C. Liu, D. Nirmalya and P. Jahanshahi, *Ind Manage Data Syst*, 120 (2020) 312.
23. R. Xiong, Y. Zhang, H. He, X. Zhou and M. G. Pecht, *IEEE Trans. Ind. Electron.*, 65 (2018) 1526.
24. W. Xu, J. Xu and X. Yan, *J. Power Electron.*, 20 (2020) 292.
25. J. Yang, Z. Peng, H. Wang, H. Yuan and L. Wu, *Int. J. Electrochem. Sci.*, 13 (2018) 4991.
26. K. Zhang, J. Ma, X. Zhao, D. Zhang and Y. He, *IEEE Access*, 7 (2019) 166657.
27. L. Zhang, H. Peng, Z. Ning, Z. Mu and C. Sun, *Appl. Sci.*, 7 (2017) 1002.
28. L. Zheng, J. Zhu, G. Wang, D. D.-C. Lu and T. He, *Energy*, 158 (2018) 1028.
29. Y. Zheng, W. Gao, M. Ouyang, L. Lu, L. Zhou and X. Han, *J. Power Sources*, 383 (2018) 50.
30. D. Liu, X. Yin, Y. Song, W. Liu and Y. Peng, *IEEE Access*, 6 (2018) 40990.
31. F. Liu, J. Ma and W. Su, *Math. Prob. Eng.*, 2019 (2019) 1.
32. Q. Miao, L. Xie, H. Cui, W. Liang and M. Pecht, *Microelectron. Reliab.*, 53 (2013) 805.
33. M. Ahwiadi and W. Wang, *IEEE Trans. Instrum. Meas.*, 68 (2019) 923.
34. X. Liu, C. Zheng, J. Wu, J. Meng, D.-I. Stroe and J. Chen, *Energies*, 13 (2020).
35. H. Zhang, Q. Miao, X. Zhang and Z. Liu, *Microelectron. Reliab.*, 81 (2018) 288.
36. J. C. Alvarez Anton, P. J. Garcia Nieto, E. Garcia Gonzalo, J. C. Viera Perez, M. Gonzalez Vega and C. Blanco Viejo, *IEEE Trans. Veh. Technol.*, 65 (2016) 4197.
37. K. Chen, S. Laghrouche and A. Djerdir, *Energy Convers. Manage.*, 195 (2019) 810.
38. H. Ebrahimzade, G. R. Khayati and M. Schaffie, *J. Mater. Cycles Waste Manage.*, 22 (2020) 228.
39. J. Feng, S. Hou, L. Yu, N. Dimov, P. Zheng and C. Wang, *Appl. Energy*, 264 (2020).
40. M. M. Hoque, M. A. Hannan and A. Mohamed, *J. Renewable Sustainable Energy*, 8 (2016).
41. K. Huang, Y.-F. Guo, Z.-G. Li, H.-C. Lin and L.-L. Li, *Math. Prob. Eng.*, (2018).
42. K. Zhang, J. Ma, X. Zhao, X. Liu and Y. Zhang, *Math. Prob. Eng.,* 2019 (2019)